arXiv:1603.00398v2 [cond-mat.mes-hall] 21 Jul 2016

Anomalous Hooke's law in disordered graphene

I.V. Gornyi[1,2,3,4], V.Yu. Kachorovskii[1,2,3,4], and A.D. Mirlin[1,3,4,5]
[1] *Institut für Nanotechnologie, Karlsruhe Institute of Technology, 76021 Karlsruhe, Germany*
[2] *A.F. Ioffe Physico-Technical Institute, 194021 St. Petersburg, Russia*
[3] *Institut für Theorie der kondensierten Materie, Karlsruhe Institute of Technology, 76128 Karlsruhe, Germany*
[4] *L.D. Landau Institute for Theoretical Physics, Kosygina street 2, 119334 Moscow, Russia*
[5] *Petersburg Nuclear Physics Institute, 188300, St.Petersburg, Russia*

(Dated: July 25, 2016)

The discovery of graphene, a single monolayer of graphite, has closed the discussion on stability of 2D crystals. Although thermal fluctuations of such crystals tend to destroy the long-range order in the system, the crystal can be stabilized by strong anharmonicity effects. This competition is the central issue of the crumpling transition, i.e., a transition between flat and crumpled phases. We show that anharmonicity-controlled fluctuations of a graphene membrane around equilibrium flat phase lead to unusual elastic properties. In particular, we demonstrate that stretching ξ of a flake of graphene is a nonlinear function of the applied tension at small tension: $\xi \propto \sigma^{\eta/(2-\eta)}$ and $\xi \propto \sigma^{\eta/(8-\eta)}$ for clean and strongly disordered graphene, respectively. Conventional linear Hooke's law, $\xi \propto \sigma$ is realized at sufficiently large tensions: $\sigma \gg \sigma_*$, where σ_* depends both on temperature and on the disorder strength.

PACS numbers: 72.80.Vp, 73.23.Ad, 73.63.Bd

Hooke's law (HL)—introduced by Robert Hooke about 350 years ago—states that the force needed to extend or compress an elastic body by some distance is proportional to that distance. Conventional theory of elasticity predicts that this law is fulfilled for low fields (in the so-called "elastic range" of tensions) and gets violated at sufficiently large tensions.

The goal of this Letter is to explore stretching of graphene, a famous two-dimensional (2D) material [1–10], as a reaction on applied tension. Measurement of the elasticity of free-standing graphene is accessible to current experimental techniques [11–15]. Remarkably, we find that, for graphene, HL fails even in the limit of the infinitesimally small tension. The underlying physics has a very close relation to the well known problem of thermodynamic stability of 2D crystals [16, 17].

Free-standing graphene is a remarkable example of an elastic crystalline 2D membrane with a high bending rigidity $\varkappa \simeq 1$ eV. The most important feature distinguishing such a membrane from conventional 2D semiconductor systems is the existence of specific type of out-of-plane phonon modes—flexural phonons (FP) [18].

In contrast to in-plane phonons with the linear dispersion, the FP are very soft, $\omega_{\mathbf{q}} \propto q^2$, and, consequently, the out-of-plane thermal fluctuations are unusually strong and tend to destroy graphene membrane by driving it into the crumpled phase [18]. The competing effect is the anharmonicity that plays here a key role.

This question was intensively discussed more than two decades ago [18–35] in connection with biological membranes, polymerized layers, and inorganic surfaces. The interest to this topic has been renewed more recently [36–43] after discovery of graphene. It was found [19–25] that the anharmonic coupling of in-plane and out-of-plane phonons stabilizes the membrane for not too high temperatures T. This is connected with a strong renormalization of the bending rigidity [24, 26, 32], $\varkappa \to \varkappa_q \propto q^{-\eta}$, for $q \to 0$, with a certain critical index η. Due to the high bare value of $\varkappa$, *clean* graphene remains flat up to all realistic temperatures. The critical exponent η was determined within several approximate analytical schemes [22, 24, 25, 32, 36]. Numerical simulations for a 2D membrane embedded in 3D space yield $\eta = 0.60 \pm 0.10$ [30] and $\eta = 0.72 \pm 0.04$ [35].

In a recent paper [44], we have developed a theory of rippling and crumpling in *disordered* free-standing graphene. We have shown that random fluctuations of the membrane curvature caused by static disorder may strongly affect properties of the membrane. We have derived coupled renormalization-group (RG) equations describing the combined flow of $\varkappa$ and disorder strength b, determined the phase diagram (flat vs. crumpled) in the $(\varkappa, b)$ plane, and explored the rippling in the flat phase.

In the present Letter, we explore the fate of HL in clean and disordered graphene. We find that linear HL breaks down both for clean and disordered cases, so that deformation of the membrane subjected to a small stretching tension $\sigma > 0$ scales as $\Delta L \propto \sigma^{\alpha}$, with a non-trivial exponent α. In the opposite case, $\sigma < 0$, $\Delta L < 0$, the membrane undergoes a buckling transition [23]. We obtain the critical index α that turns out to be different for clean and disordered cases. Our findings imply that for sufficiently strong disorder the anomalous elasticity of graphene is fully determined by static random deformations—ripples. The non-linearity of elasticity of graphene found in this work is in agreement with recent experimental findings [14, 15]. Related theoretical results have been recently obtained for clean membranes in the ribbon geometry [45] and by numerical simulations [46].

We consider a $2D$ membrane embedded in the d-

dimensional space ($d > 2$). The starting point of our analysis is the energy functional

$$E=\int d^2x\left[\frac{\varkappa}{2}(\Delta\mathbf{r})^2+\frac{\mu}{4}(\partial_\alpha\mathbf{r}\partial_\beta\mathbf{r}-\delta_{\alpha\beta})^2+\frac{\lambda}{8}(\partial_\gamma\mathbf{r}\partial_\gamma\mathbf{r}-D)^2\right]$$

which can be obtained from the general gradient expansion of elastic energy [21] by using a certain rescaling of coordinates (see discussion in [44]). Here $\varkappa$ is the bare bending rigidity, while μ and λ are in-plane coupling constants. The $d-$dimensional vector $\mathbf{r} = \mathbf{r}(\mathbf{x})$ describes a point on the membrane surface and depends on the $2D$ coordinate $\mathbf{x}$ that parametrizes the membrane. The vector $\mathbf{r}$ can be split into $\mathbf{r} = \xi\mathbf{x} + \mathbf{u} + \mathbf{h}$, where vectors $\mathbf{u} = (u_1, u_2)$, $\mathbf{h} = (h_1, ..., h_{d_c})$ represent in-plane and out-of-plane displacements, respectively, and $d_c = d - 2$. The stretching factor ξ is equal to unity in the mean-field approximation but gets reduced due to fluctuations. In terms of $\mathbf{u}$, $\mathbf{h}$, and ξ, the energy becomes

$$E=\frac{L^2(\mu+\lambda)(\xi^2-1)}{2}\left[\xi^2-1+\int\frac{d^2\mathbf{x}}{L^2}\partial_\alpha\mathbf{h}\partial_\alpha\mathbf{h}\right]+E_0, \quad (1)$$

where $\tilde{\mathbf{u}} = \xi\mathbf{u}$ and $E_0 = E_0(\tilde{\mathbf{u}}, \mathbf{h})$ describes the energy of in-plane and out-of-plane fluctuation. We proceed now to include the static disorder. As shown in Ref. [44], the relevant disorder is produced by a random curvature. The energy of fluctuations including such disorder reads [28]

$$E_0(\mathbf{u},\mathbf{h}) = \int d^Dx\left\{\frac{\varkappa}{2}(\Delta\mathbf{h}+\boldsymbol{\beta})^2+\mu u_{ij}^2+\frac{\lambda}{2}u_{ii}^2\right\}. \quad (2)$$

Here $u_{\alpha\beta} = (\partial_\alpha u_\beta + \partial_\beta u_\alpha + \partial_\alpha\mathbf{h}\partial_\beta\mathbf{h})/2$ is the strain tensor and $\boldsymbol{\beta} = \boldsymbol{\beta}(\mathbf{x})$ is a random vector with Gaussian distribution $P(\boldsymbol{\beta}) = Z_{\boldsymbol{\beta}}^{-1}\exp\left[-(1/2b)\int\beta^2(\mathbf{x})d^D\mathbf{x}\right]$, where b is the disorder strength and $Z_{\boldsymbol{\beta}}$ is a normalization factor. For $\boldsymbol{\beta} = 0$, $E_0(\mathbf{u}, \mathbf{h})$ coincides with the conventional expression for elastic energy of nearly flat membrane [18].

The second term in the square brackets in Eq. (1) describes the coupling between fluctuations and stretching. Such a coupling leads to shrinking of the membrane in the $x-$plane. As a result, the optimal value of ξ deviates from the mean-field value $\xi = 1$ due to the fluctuations. The size of the membrane with fluctuations R is related to the size L of the membrane without fluctuations as follows: $R = \xi L$. Hence, the "projected" area of the membrane reads $A = \xi^2L^2$.

For $\sigma = 0$, the equilibrium value of ξ reads [44, 47]:

$$\xi^2 = 1 - \langle\partial_\alpha\mathbf{h}\partial_\alpha\mathbf{h}\rangle/2. \quad (3)$$

Here angular brackets denote the Gibbs averaging. Application of tension σ to the membrane leads to the increase of ξ^2, as compared to Eq. (3). Below we calculate function $\xi(\sigma)$, both for clean and disordered cases.

Clean case ($b = 0$). For $\sigma \neq 0$, the propagator of $h-$modes calculated in the harmonic approximation is given by (see [47] for technical details)

$$\langle h_{\mathbf{q}}^\alpha h_{-\mathbf{q}'}^\beta\rangle = (2\pi)^2\delta(\mathbf{q}-\mathbf{q}')\ \delta_{\alpha\beta}\ G_{\mathbf{q}}^0, \quad (4)$$

where $G_{\mathbf{q}}^0 = T/(\varkappa q^4 + \sigma q^2)$. Tension σ is given by a derivative of the free energy F with respect to A [25], $\sigma = \partial F/\partial A$, and is related to ξ as [47]

$$\sigma = (\mu+\lambda)\left(\xi^2 - 1 + \langle\partial_\alpha\mathbf{h}\partial_\alpha\mathbf{h}\rangle/2\right). \quad (5)$$

Conventional HL can be derived from Eq. (5) by neglecting the contribution of fluctuations and assuming that ξ is close to unity: $\sigma_{\rm conv} \approx k_0\,(\xi - 1)$. Here $k_0 = 2(\mu+\lambda) \approx 400$ N/m is in-plane stiffness predicted for flat graphene [48, 49] and measured in Refs. [11, 12]. The main purpose of the further discussion is to demonstrate that the contribution of fluctuations is of crucial importance, so that this law fails in the limit $\sigma \to 0$ where stretching turns out to be a nonlinear function of σ.

For large momenta, $q > q_\sigma$, where $q_\sigma = \sqrt{\sigma/\varkappa}$, Green's function is approximately given by $G_{\mathbf{q}}^0 = T/\varkappa q^4$. The strong infrared singularity $G_{\mathbf{q}}^0 \propto 1/q^4$ leads to a logarithmic divergence of $\langle\partial_\alpha\mathbf{h}\partial_\alpha\mathbf{h}\rangle$ and, consequently, in view of Eq. (3), to the renormalization of ξ [44]. Hence, ξ becomes scale-dependent: $\xi \to \xi_L$, where $L \sim q^{-1}$. At finite q, the renormalization is stopped because of the term σq^2 in the denominator of $G_{\mathbf{q}}^0$. To determine the q-dependence of the renormalization of ξ, one should take into account that the bending rigidity is also renormalized for sufficiently small wave vectors $q \ll q_*$ according to the RG equation [24, 26, 32],

$$d\varkappa/d\Lambda = \eta\varkappa \ \ \Rightarrow \ \ \varkappa_q = \varkappa\,(q_*/q)^\eta. \quad (6)$$

Here $\Lambda = \ln(q_*/q)$, η is the anomalous dimension of the bending rigidity, q_* is the inverse Ginzburg length,

$$q_* \simeq \sqrt{\tilde{\mu}\ T}/\varkappa, \quad (7)$$

and $\tilde{\mu} = 3\mu(\mu+\lambda)/[8\pi(2\mu+\lambda)]$, see Ref. [44]. Below, we assume that $q_* \gg q_\sigma$. In this case, a competition between the two terms in the denominator of $G_{\mathbf{q}}^0$ leads to appearance of a new spatial scale $\tilde{q}_\sigma$ determined by the condition $\varkappa_q q^2 = \sigma$, yielding $\tilde{q}_\sigma = q_\sigma\,(q_\sigma/q_*)^{\eta/(2-\eta)}$. Next, we calculate $\langle\partial_\alpha\mathbf{h}\partial_\alpha\mathbf{h}\rangle$ with the use of Eq. (6) and substitute it in Eq. (5) (see [47] for details). This yields an equation that determines the dependence of $\xi = \xi_{L\to\infty}$ on σ,

$$\frac{\sigma}{\mu+\lambda} = \xi^2 - 1 + \frac{d_cT}{4\pi}\int_0^{q_{\rm uv}}\frac{qdq}{\varkappa_q q^2+\sigma}, \quad (8)$$

where $q_{\rm uv}$ is the ultraviolet cutoff ($q_{\rm uv} \gg q_*$). In the absence of stress ($\sigma = 0$), Eq. (8) simplifies. For $d_c \gg 1$, when $\eta = 2/d_c$, one gets [22, 44]

$$\xi^2|_{\sigma=0} \equiv \xi_0^2 = 1 - \varkappa_{\rm cr}/\varkappa = 1 - T/T_{\rm cr}, \quad (9)$$

where $\varkappa_{\rm cr} = d_c^2 T/8\pi$ and $T_{\rm cr} = 4\pi\eta\varkappa/d_c$ is the temperature of crumpling transition (CT) for a given value of bare bending rigidity $\varkappa$. For $T < T_{\rm cr}$, the stretching factor is finite, $\xi_0 > 0$, and the membrane is in the flat phase. For $T > T_{\rm cr}$, the membrane undergoes the CT, so that $\xi \to 0$ for $L < \infty$. Interestingly, Eq. (9) predicts a negative expansion coefficient of the membrane, $d\xi_0/dT < 0$.

For $\sigma \neq 0$, we assume for simplicity $d_c = 1$, $\mu \sim \lambda \sim k_0$, (this is the case for graphene) and rewrite Eq. (8) as follows (see derivation in [47])

$$\frac{2\sigma_*}{k_0}\left[\frac{\sigma}{\sigma_*} + \frac{1}{\alpha}\left(\frac{\sigma}{\sigma_*}\right)^{\alpha}\right] = \xi^2 - \xi_0^2, \tag{10}$$

where

$$\alpha = \eta/(2-\eta), \quad \sigma_* = Ck_0T/T_{\rm cr}, \tag{11}$$

and $C \sim 1$ is a numerical coefficient. Equation (10) represents a general form of HL for clean membrane. The l.h.s. of this equation contains two terms: a regular term, proportional to σ, and an irregular one that shows a fractional scaling with σ. Analytical approximations [32], as well as numerical simulations [30, 35] for the physical case $D = 2$, $d = 3$, show that $\eta \simeq 0.7$, yielding $\alpha \simeq 0.54 < 1$. Hence, the irregular term dominates at small σ, and ξ shows an anomalous behavior, while the linear HL, $d\sigma/d\xi = k_0$, is realized for sufficiently large tensions, $\sigma \gg \sigma_*$. For sufficiently low temperatures, $T \ll T_{\rm cr}$, the stretching corresponding to σ_* is small, $\xi_* - \xi_0 \sim T/T_{\rm cr} \ll 1$. For $\sigma > \sigma_*$, the term $(\sigma/\sigma_*)^\alpha$ becomes subleading. (In this case $\tilde{q}_\sigma$ turns out to be larger than q_*, which leads to additional suppression of this term, $\alpha^{-1}(\sigma/\sigma_*)^\alpha \to \ln(\sigma/\sigma_*)$ [47]). One may introduce two exponents, governing the stretching in the anomalous regime. Far from the transition point ($T < T_{\rm cr}$), one can expand $\xi^2 - \xi_0^2 \approx 2(\xi - \xi_0)\xi_0$, thus finding

$$\xi - \xi_0 \propto \sigma^\alpha, \ \text{ far from CT point.} \tag{12}$$

Exactly at the transition point $T = T_{\rm cr}$, $\xi_0 = 0$ and

$$\xi \propto \sigma^{\alpha/2}, \quad \text{at the CT point.} \tag{13}$$

The above results can be easily generalized to an arbitrary dimensionality of the membrane, $D > 2$, by replacing $d^2\mathbf{q} \to d^D\mathbf{q}$ in Eq. (8). This leads to the replacement $\alpha \to (D-2+\eta)/(2-\eta)$ of the critical index in Eqs. (10), (12) and (13) . The latter equation for α was obtained previously in Refs. [23, 25] for $\eta = 0$, which corresponds to the case $d_c = \infty$ [50], and predicted in [26] from scaling considerations. As seen from Eq. (10), the tension leads to an increase of $T_{\rm cr}$ and, respectively, to a decrease of $\varkappa_{\rm cr}$. Indeed, setting $\xi = 0$ in Eq. (10) and assuming that $\sigma \ll \sigma_*$, we find the tension-induced change of the critical temperature, $\delta T_{\rm cr}/T_{\rm cr} = -\delta\varkappa_{\rm cr}/\varkappa_{\rm cr} \sim (\sigma/k_0)^\alpha$.

Disordered case. The derivation of perturbative RG equations for disordered graphene is performed by using replica trick within RPA scheme, in analogy with the case $\sigma = 0$ studied in Ref. [44]. Technical details of calculations are presented in [47]. First, we find $\overline{\langle \partial_\alpha \mathbf{h} \partial_\alpha \mathbf{h}\rangle}$ in the harmonic approximation:

$$\overline{\langle \partial_\alpha \mathbf{h} \partial_\alpha \mathbf{h}\rangle} = \int \frac{d^2\mathbf{q}}{(2\pi)^2} \frac{d_c\, T}{\varkappa q^2 + \sigma}\left[1 + f\frac{\varkappa q^2}{\varkappa q^2 + \sigma}\right]. \tag{14}$$

Here the overbar denotes the disorder averaging and $f = b\varkappa/T$ is a dimensionless parameter characterising the ratio of disorder to thermal fluctuations. For fixed $\varkappa$ and f, the integral in Eq. (14) logarithmically diverges for $\varkappa q^2 \gg \sigma$ and saturates for $\varkappa q^2 \ll \sigma$. In view of Eq. (3), we conclude that ξ is renormalized:

$$\frac{d\xi^2}{d\Lambda} \approx -\frac{d_c}{4\pi}\frac{T}{\varkappa}(1+f), \quad \text{for } q \gg \tilde{q}_\sigma, \tag{15}$$

and $d\xi^2/d\Lambda = 0$ for $q \ll \tilde{q}_\sigma$. The Ginzburg scale q_* is also affected by disorder [44]: $q_* \sim \sqrt{\tilde{\mu}T(1+2f)}/\varkappa$. For strong disorder or low temperatures, $f \gg 1$, we find that

$$q_* \sim \sqrt{\tilde{\mu}b/\varkappa} \tag{16}$$

is independent of temperature, while for weak disorder ($f \ll 1$), we recover Eq. (7), $q_* \propto T^{1/2}$. Below we show that $\tilde{q}_\sigma$ is also modified by sufficiently strong disorder.

In the harmonic approximation, $\varkappa$ and f are constants. However, they become scale-dependent due to the coupling between in-plane and out-of-plane fluctuations: $\varkappa \to \varkappa_q$ and $f \to f_q$. For $q \gg \tilde{q}_\sigma$, corresponding RG equations were derived in Ref. [44] [see also Eq. (S38) of [47]]. For strong disorder, $f \gg 1$, the RG equations look: $d\varkappa/d\Lambda = \eta\varkappa/4$ and $df/d\Lambda = -3\eta/4$. The first equation yields $\varkappa_q = \varkappa(q_*/q)^{\eta/4}$. Equating $\varkappa_q q^2$ to σ, we find:

$$\tilde{q}_\sigma = q_\sigma\,(q_\sigma/q_*)^{\eta/(8-\eta)}, \tag{17}$$

where q_* is given by Eq. (16). Since $\varkappa$ changes faster than f, one can set $f = \text{const}$ in Eq. (15). Using Eq. (5), we find that the equation that determines the dependence of ξ on σ for a strongly disordered membrane is given by Eq. (10) with $\xi_0^2 = 1 - B$,

$$\alpha = \eta/(8-\eta) \simeq 0.1, \quad \text{and} \quad \sigma_* = C' k_0 B, \tag{18}$$

where $B = bd_c^2/2\pi$ and $C' \sim 1$ is a numerical coefficient. Note that the temperature drops out from the Hooke's law for disordered membrane. For $\sigma = 0$, the CT ($\xi = 0$) corresponds to $B = B_{\rm cr} = 1$, in agreement with previous study (see Fig. 5 of Ref. [44]). For $B \ll B_{\rm cr}$ the stretching corresponding to σ_* reads $\xi_* - \xi_0 \sim B/\alpha$. The tension enhances the critical value of disorder: $\delta B_{\rm cr} \equiv B_{\rm cr} - 1 \sim \alpha^{-1}(\sigma/k_0)^\alpha$. The anomalous stress-strain relations have the form (12) and (13) for $B < B_{\rm cr}$ and $B = B_{\rm cr}$, respectively, with appropriate replacement of α: the "clean" value (11) is replaced

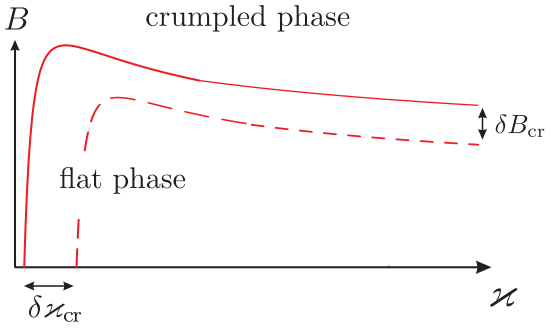

FIG. 1: Phase diagram of graphene in the plane of parameters $\varkappa$ (bending rigitidy) and B (disorder) at non-zero tension σ. The CT separating crumpled and flat phases is shown by full red line; dashed line represents the CT for $\sigma = 0$ [44].

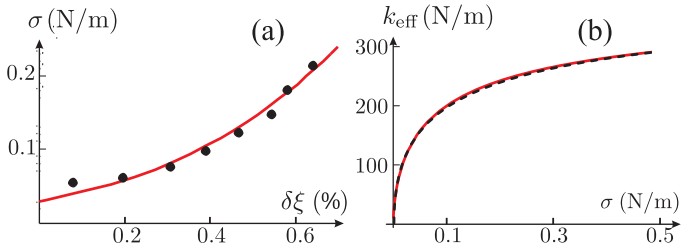

FIG. 2: (a) Stress-strain dependence. Dots – experiment [15], line – theory for strongly disordered case $\alpha = 0.1$ with degree of disorder $B = 0.004$. (b) Effective stiffness $k_{\rm eff}$ *vs.* stress σ in clean graphene at $T = 300$K. Dashed line – numerical simulations [46], solid line – Eq. (19) with $\alpha = 0.62$ (i.e., $\eta = 0.765$) and $\sigma_* \simeq 0.1\,$N/m.

by the considerably smaller "dirty" value (18). Hence, stretching of a strongly disordered membrane is a nonlinear function of a weak tension, just as in the clean case. However, the corresponding power-law exponents differ from that of a clean system. As in the clean case, the conventional HL is restored for $\sigma \gg \sigma_*$.

The RG flow for ξ stops at $q \sim \tilde{q}_\sigma$. Thus, if $\xi > 0$ at this scale, the system is in the flat phase. Conversely, if ξ becomes zero before $\tilde{q}_\sigma$ is reached, the membrane crumples. The phase diagram in the parameter plane $(\varkappa, B)$, as obtained by numerical solution of RG equations, is shown in Fig. 1. The tension shifts the line separating the flat and crumpled phases; this shift is characterized by $\delta\varkappa_{\rm cr}$ and $\delta B_{\rm cr}$. Interestingly, the RG flows for $\varkappa$ and f do not stop at the point $q \sim \tilde{q}_\sigma$ [47]. However, for smaller q, such that $\varkappa_q q^2 \ll \sigma$, the scaling of $\varkappa$ is irrelevant for the CT and the membrane remains flat.

Both in the clean and disordered case, it is convenient to introduce the effective stiffness

$$k_{\rm eff} = \partial\sigma/\partial\xi \simeq k_0 \frac{(\sigma/\sigma_*)^{1-\alpha}}{1+(\sigma/\sigma_*)^{1-\alpha}}. \qquad (19)$$

It is strongly reduced for a weak strain ($\sigma \ll \sigma_*$), vanishing at the point of the buckling transition ($\sigma = 0$).

Let us now discuss characteristic values of parameters for the case of graphene. In Ref. [44] we estimated the amplitude of the static disorder as $b = 0.03$ based on experimental measurements of parameters of ripples [51]. Taking the bare value of the bending rigidity for graphene, $\varkappa \simeq 1$ eV, we find $f \simeq 1$ at room temperature. This implies that at $T \simeq 300\,$K the system is in the crossover regime between the clean and disordered limits. In this regime, the exponent α takes a non-universal value between the clean ($\alpha \simeq 0.5$) and disordered ($\alpha \simeq 0.1$) values. For low low temperatures, $T \ll 300\,$K, we predict then the disordered value $\alpha \simeq 0.1$, while for elevated temperatures the clean value $\alpha \simeq 0.5$ should be reached. (In fact, α flows as a function of σ, tending to the clean value $\simeq 0.5$ for smallest strains. This flow is, however, logarithmically slow and may be difficult to observe experimentally.) Clearly, the crossover temperature may vary depending on sample preparation (degree of disorder). For clean samples, we estimate the crossover tension and stretching at $T \simeq 300\,$K from Eq. (11), yielding $\sigma_* \simeq 1\,$N/m and $\xi_* - \xi_0 \simeq 0.003$ (for $\eta = 0.7$ and $C = 1$). For disorder-dominated samples with the above disorder strength $b = 0.03$, we get $B \simeq 0.005$, which yields, according to (18), an estimate $\sigma_* \simeq 2\,$N/m and $\xi_* - \xi_0 \simeq 0.05$ (for $C' = 1$).

Our results compare well with a recent detailed experimental study of graphene elasticity [15]. It was found there that the room-temperature in-plane stiffness of graphene is reduced compared to its value k_0 for "ideal" graphene (no disorder, $T = 0$) by a large factor (up to ~ 40) at low stretching. When temperature was lowered down to 10 K, the stiffness showed a sizeable increase, still remaining much smaller than 400 N/m. These data are in agreement with our conclusion that ripples and FP strongly weaken the in-plane stiffness, yielding comparable contributions at room temperature. In Fig. 2a we compare our theory with the strain-stress dependence presented in Fig. 2c of Ref. [15]. We use Eq. (10) describing both clean and disorder case with the appropriate choice of α and σ_*, considering α and σ_* as fitting parameters. The solid lines in In Fig. 2a show dependence of σ on $\delta\xi = \xi(\sigma) - \xi(\sigma_0)$, where σ_0 is built-in stress extracted from experimental data [15]. The best fit is achieved for $\alpha \approx 0.1$ and $\sigma_* \approx 1.68$ N/m. The obtained value of α implies that the sample is in the disorder-dominated regime, with the degree of disorder $B \simeq 0.004$ (we set the numerical coefficient $C' = 1$ here). This estimate is in agreement with the value $B = 0.005$ [44] obtained from the transmission-electron-microscopy data of Refs. [51, 52]. For a more detailed comparison with experiment, measurements of strain-stress curves in a wide range of temperatures would be of great interest.

Our results also compare very well with numerical simulations of Ref. [46] which were performed for clean graphene. In particular, the scaling of $k_{\rm eff}$ for $f \ll 1$

is in an excellent agreement with the large-sample data (number of atoms 37888). For comparison, we used the empirical formula (11) of Ref. [46] which perfectly fits numerical data obtained there (see [47] for details). As seen from Fig. 2b, the numerical data are very well described by our Eq. (19) with $\alpha \simeq 0.62$ ($\eta \simeq 0.76$), as expected in the clean limit. The comparison to the results of numerical simulations allows us to determine the numerical coefficient C in Eq. (11), which turns out to be $C \approx 0.093$. The corresponding crossover stress and strain values read $\sigma_* \simeq 0.1\,\mathrm{N/m}$ and $\xi_* - \xi_0 \simeq 0.0006$, respectively.

To conclude, the theory of anomalous Hooke's law has been developed, for both clean and disordered graphene. In both cases, scaling of the deformation with the external force obeys a fractal power law in the limit of weak forces. This behavior is dominated by thermal fluctuations for clean graphene, while for strongly disordered graphene it is governed by static ripples. Remarkably, the same coupling between longitudinal and transverse modes that enhances the bending rigiditiy, thus rescuing the flat phase of the membrane, leads simultaneously to a dramatic softening of the in-plane elasticity.

We thank M.I. Katsnelson for useful comments, and K. Bolotin and R. Nicholl for providing us with experimental data of Ref. [15] and stimulating discussions. The work was supported by the Russian Science Foundation (grant No. 14-42-00044).

[1] K.S. Novoselov, A.K. Geim, S.V. Morozov, D. Jiang, Y. Zhang, S.V. Dubonos, I.V. Grigorieva and A.A. Firsov, Science **306**, 666 (2004).
[2] K.S. Novoselov, A.K. Geim, S.V. Morozov, D. Jiang, M.I. Katsnelson, I.V. Grigorieva, S.V. Dubonos and A.A. Firsov, Nature **438**, 197 (2005).
[3] Y. Zhang, Y.-W. Tan, H.L. Stormer and P. Kim, Nature **438**, 201 (2005).
[4] A.K. Geim and K.S. Novoselov, Nature Materials **6**, 183 (2007).
[5] A.H. Castro Neto, F. Guinea, N.M.R. Peres, K.S. Novoselov, and A.K. Geim, Rev. Mod. Phys. **81**, 109 (2009).
[6] S. Das Sarma, S. Adam, E. H. Hwang, and E. Rossi, Rev. Mod. Phys. **83**, 407 (2011).
[7] V.N. Kotov, B. Uchoa, V.M. Pereira, F. Guinea, and A. H. Castro Neto, Rev. Mod. Phys. **84**, 1067 (2012).
[8] M.I. Katsnelson, *Graphene: Carbon in Two Dimensions Hardcover*, Cambridge University Press (2012).
[9] E. L. Wolf, *Graphene: A New Paradigm in Condensed Matter and Device Physics*, Oxford University Press (2014).
[10] L.E.F. Foa Torres, S. Roche, J.-C. Charlier, *Introduction to Graphene-Based Nanomaterials From Electronic Structure to Quantum Transport*, Cambridge University Press (2014).
[11] C. Lee, X. Wei, J.W. Kysar, J. None, Science **321**, 385 (2008).
[12] D. Metten, F. Federspiel, M. Romeo, S. Berciaud, Phys. Rev. Applied **2**, 054008 (2014).
[13] M. K. Blees, A.W. Barnard, P. A. Rose, S. P. Roberts, K. L. McGill, P. Y. Huang, A. R. Ruyack, J. W. Kevek, B. Kobrin, D.A. Muller, and P. L. McEuen, Nature **524**, 204 (2015).
[14] G. Lopez-Polin, C. Gomez-Navarro, V. Parente, F. Guinea, M. I. Katsnelson, F. Perez-Murano, and J. Gomez-Herrero, Nature Physics **11**, 26 (2015); G. Lopez-Polin, M. Jaafar, F. Guinea, R. Roldan, C. Gomez-Navarro, and J. Gomez-Herrero, arXiv:1504.05521.
[15] R.J.T. Nicholl, H. J. Conley, N. V. Lavrik, I. Vlassiouk, Y. S. Puzyrev, V. P. Sreenivas, S. T. Pantelides, and K. I. Bolotin, Nature Communications 6:8789 doi: 10.1038/ncomms9789 (2015).
[16] N. D. Mermin and H. Wagner, Phys. Rev. Lett. **17**, 1133 (1966).
[17] L.D. Landau and E.M. Lifshitz, *Statistical Physics, Part I* (Pergamon Press, Oxford, 1980).
[18] D. Nelson, T. Piran, and S. Weinberg (Eds.) *Statistical Mechanics of Membranes and Surfaces* (World Scientific, Singapore, 1989).
[19] D.R. Nelson and L. Peliti, J. Phys. (Paris) **48**, 1085 (1987).
[20] Y.Kantor and D.R. Nelson, Phys. Rev. Lett. **58**, 2774 (1987); Phys. Rev. A **36**, 4020 (1987);
[21] M. Paczuski, M. Kardar, and D.R. Nelson, Phys. Rev. Lett. **60**, 2638 (1988).
[22] F. David and E. Guitter, Europhys. Lett. **5**, 709 (1988).
[23] E. Guitter, F. David, S. Leibler, and L. Peliti, Phys. Rev. Lett. **61**, 2949 (1988).
[24] J.A. Aronovitz and T.C. Lubensky, Phys. Rev. Lett. **60**, 2634 (1988).
[25] E. Guitter, F. David, S. Leibler, and L. Peliti, J.Phys. France **50** 1787 (1989).
[26] J. Aronovitz, L. Golubović, and T.C. Lubensky, J.Phys. France **50** 609 (1989).
[27] M. Paczuski and M. Kardar, Phys. Rev. A **39**, 6086 (1989).
[28] L. Radzihovsky and D.R. Nelson, Phys. Rev. A **44**, 3525 (1991).
[29] D.R. Nelson and L. Radzihovsky, Europhys. Lett. **16**, 79 (1991).
[30] G. Gompper and D.M. Kroll, Europhys. Lett. **15**, 783 (1991).
[31] L. Radzihovsky and P. Le Doussal, J.Phys. I France **2** 599 (1992).
[32] P. Le Doussal and L. Radzihovsky, Phys. Rev. Lett **69**, 1209 (1992).
[33] D.C. Morse, T.C. Lubensky, and G.S. Grest, Phys. Rev. A **45**, R2151 (1992).
[34] P. Le Doussal and L. Radzihovsky, Phys. Rev. B **48**, 3548 (1993).
[35] M.J. Bowick, S.M. Catterall, M. Falcioni, G. Thorleifsson, and K.N. Anagnostopoulos, J. Phys. I France **6**, 1321 (1996).
[36] J.-P. Kownacki, and D. Mouhanna, Phys. Rev. E **79**, 040101(R) (2009).
[37] D. Gazit, Phys. Rev. E **80**, 041117 (2009).
[38] D. Gazit, Phys. Rev. B **80**, 161406(R) (2009).
[39] F.L. Braghin and N. Hasselmann , Phys. Rev. B **82**, 035407 (2010).
[40] V.V. Lebedev and E.I. Kats, Phys. Rev. B **85**, 045416 (2012).

[41] E.I. Kats and V.V. Lebedev, Phys. Rev. B **89**, 125433 (2014).
[42] B. Amorim, R. Roldán, E. Cappelluti, A. Fasolino, F. Guinea, and M. I. Katsnelson, Phys. Rev. B **89**, 224307 (2014).
[43] E. I. Kats and V. V. Lebedev, Phys. Rev. E **91**, 032415 (2015).
[44] I.V. Gornyi, V. Yu. Kachorovskii, and A. D. Mirlin, Phys. Rev. B **92**, 155428 (2015).
[45] A. Kosmrlj and D. R. Nelson, arXiv:1508.01528.
[46] J. H. Los, A. Fasolino, and M. I. Katsnelson, Phys. Rev. Lett. **116**, 015901 (2016).
[47] See Supplemental Material for technical details.
[48] J.W. Jiang, J.S. Wang, B. Li, Phys. Rev. B **80**, 113405 (2009).
[49] M.M. Shokrieh, R. Rafiee, Mater. Design **31**, 790 (2010).
[50] In these papers, HL was written in terms of tension $\sigma' = L^{-2}\partial F/\partial\xi = 2\xi\sigma$.
[51] D. A. Kirilenko, A. T. Dideykin, and G. Van Tendeloo, Phys. Rev. B **84**, 235417 (2011).
[52] J.C. Meyer, A.K. Geim, M.I. Katsnelson, K.S. Novoselov, T.J. Booth and S. Roth, Nature **446**, 60 (2007).

SUPPLEMENTAL MATERIAL

Derivation of the free energy of the clean membrane with nonzero tension

We start with Eq. (1) of the main text for the elastic energy (in the absence of disorder, $\boldsymbol{\beta} = 0$) and rewrite it as follows

$$E = \frac{L^2(\mu+\lambda)}{2}\left[\left(\xi^2 - 1 + \frac{K}{2}\right)^2 - \frac{K^2}{4}\right] + E_0(\tilde{\mathbf{u}}, \mathbf{h}), \tag{S.1}$$

where

$$K = \int \frac{d^2x}{L^2}\partial_\alpha \mathbf{h}\partial_\alpha \mathbf{h} \tag{S.2}$$

and $E_0(\tilde{\mathbf{u}}, \mathbf{h})$ is given by Eq. (2) of the main text (with $\boldsymbol{\beta} = 0$). Next, we calculate the free energy F from the partition function Z that is written as a functional integral over fluctuations $\tilde{\mathbf{u}}, \mathbf{h}$:

$$F = -T\ln Z, \tag{S.3}$$

$$Z = \int e^{-E/T}\{d\tilde{\mathbf{u}}d\mathbf{h}\}. \tag{S.4}$$

As a first step, one can integrate out the in-plane modes $\tilde{\mathbf{u}}$, thus obtaining the energy functional that depends on $\mathbf{h}$ fields only [32, 44]. The interaction between these fields is described by the quartic term $R_{\mathbf{q}}(\mathbf{k},\mathbf{k}')(\mathbf{h}_{\mathbf{k}+\mathbf{q}}\mathbf{h}_{-\mathbf{k}})(\mathbf{h}_{-\mathbf{k}'-\mathbf{q}}\mathbf{h}_{\mathbf{k}'})$ (the explicit form of $R_{\mathbf{q}}(\mathbf{k},\mathbf{k}')$ can be found in Refs. [32, 44]). This interaction can be taken into account within the RPA approach. It is screened by polarization bubbles and leads to the renormalization of the bending rigidity: $\varkappa \to \varkappa_q$. The term with $q = 0$ (zero-mode) needs special attention.

There are two zero-mode contributions: the term

$$E^{(2)}_{ZM} = -\frac{L^2(\mu+\lambda)K^2}{8} = -\frac{\mu+\lambda}{8L^2}\left[\int (dQ)Q^2(\mathbf{h}_{-\mathbf{Q}}\mathbf{h}_{\mathbf{Q}})\right]^2 \tag{S.5}$$

[see Eq. (S.1)], and the term with $q = 0$ coming from the h^4-terms in $E_0(\tilde{\mathbf{u}}, \mathbf{h})$:

$$E^{(4)}_{ZM} = \int \frac{(dQ)(dQ')}{L^2}\left[\frac{\mu}{4}(\mathbf{QQ}')^2 + \frac{\lambda}{8}Q^2Q'^2\right] \times (\mathbf{h}_{-\mathbf{Q}}\mathbf{h}_{Q})(\mathbf{h}_{-\mathbf{Q}'}\mathbf{h}_{\mathbf{Q}'}) \tag{S.6}$$

[here $(dQ) = d^2\mathbf{Q}/(2\pi)^2$]. Note that the h^4-contribution arising after integrating terms of the type $\tilde{u}h^2$ over $\{d\tilde{u}\}$ does not contain the $q = 0$ term because the zero mode of the in-plane fluctuations, $\xi\mathbf{x}$, was separated from the very beginning. Combining the contributions (S.5) and (S.6), we find

$$E_{ZM} = \frac{\mu}{4L^2}\int (dQ)(dQ')\left[(\mathbf{QQ}')^2 - \frac{Q^2Q'^2}{2}\right] \times (\mathbf{h}_{-\mathbf{Q}}\mathbf{h}_{Q})(\mathbf{h}_{-\mathbf{Q}'}\mathbf{h}_{\mathbf{Q}'}). \tag{S.7}$$

One can calculate the "Hartree" and "Fock" contributions to the self-energy coming from the functional (S.7). The Hartree contribution vanishes after averaging over the angle between $\mathbf{Q}$ and $\mathbf{Q}'$. The Fock contribution comes from $\mathbf{Q} = \mathbf{Q}'$ and hence survives the angular averaging. The lowest-order Fock correction to the self-energy is momentum-independent, but is inversely proportional to the system size: $\Sigma \propto \varkappa q_*^2/L^2$, thus vanishing in the thermodynamic limit. Taking screening into account leads to a further suppression of the Fock self-energy. Indeed, the inverse polarization operator increases with decreasing q : $\Pi_{\mathbf{q}}^{-1} \propto q^2$, see Eq. (38) of Ref. [44]. Since the interaction line in the zero-mode terms carries zero momentum, we take polarization operator at $q \sim 1/L$ and finally obtain: $\Sigma \propto \varkappa/L^4$. Thus, the zero-mode interaction can be safely neglected. It is worth noting that the key point of this derivation is the cancellation of the Hartree contribution after the angular averaging. Indeed, one can check that each of the two terms of the opposite sign in Eq. (S.7) yields a correction to self-energy in the Hartree channel which does not depend on the system volume.

We are, therefore, left with the following effective functional

$$E = \frac{L^2(\mu+\lambda)}{2}\left(\xi^2 - 1 + \frac{K}{2}\right)^2 + \int (dq)\frac{\varkappa_q}{2}q^4 h_{\mathbf{q}}h_{-\mathbf{q}}. \tag{S.8}$$

Since the in-plane modes are integrated out, the partition function, Eq. (S.4), contains now the integral over $\{d\mathbf{h}\}$ only. To do this integration, we first introduce an integral over an auxiliary field χ,

$$\exp\left[-\frac{L^2(\mu+\lambda)}{2T}\left(\xi^2 - 1 + \frac{K}{2}\right)^2\right] = \frac{L}{\sqrt{2\pi(\mu+\lambda)T}} \times \int d\chi \exp\left\{-\left[\frac{\chi^2}{2(\mu+\lambda)} - i\chi\left(\xi^2 - 1 + \frac{K}{2}\right)\right]\frac{L^2}{T}\right\}.$$

Next, we calculate the Gaussian integral over $\{d\mathbf{h}\}$ and get (omitting irrelevant constants)

$$F = -T\ln\left[\int d\chi \exp\left(-\frac{L^2 S}{T}\right)\right], \tag{S.9}$$

where

$$S = S(\chi,\xi) = \frac{\chi^2}{2(\mu+\lambda)} - i\chi(\xi^2 - 1) + \frac{d_c T}{2}\int (dq)\ln(\varkappa_q q^2 - i\chi). \tag{S.10}$$

The stationary phase condition, $\partial S/\partial\chi = 0$, for the integral in Eq. (S.19) yields

$$\chi = \chi_0 = i\sigma, \tag{S.11}$$

where σ is related to ξ by Eq. (8) of the main text. Calculating the integral over $d\chi$, we find

$$F = -\frac{\sigma^2 L^2}{2(\mu+\lambda)} + \sigma L^2(\xi^2-1) + \frac{d_c T}{2}\sum_{\mathbf{q}} \ln(\sigma + \varkappa_q q^2). \tag{S.12}$$

Here we omitted terms independent on ξ and σ as well as terms, which are small with respect to the system size. Differentiating Eq. (S.12) with respect to the projected area $A = \xi^2 L^2$ yields $\sigma = \partial F/\partial A$ as it should be. For $\sigma \neq 0$, the Green function of the out-of-plane modes reads

$$\langle h^{\alpha}_{\mathbf{q}} h^{\beta}_{-\mathbf{q}'}\rangle = (2\pi)^2 \delta_{\alpha\beta}\ \delta(\mathbf{q}-\mathbf{q}')\frac{T}{\varkappa_q q^4 + \sigma q^2}. \tag{S.13}$$

Here the angular brackets $\langle\cdots\rangle$ denote the Gibbs averaging with the weight $Z^{-1}\exp(-E/T)\{d\mathbf{h}\}$ and E is given by Eq. (S.8).

Derivation of Eq. (10) of the main text

Rewriting integral in the r.h.s. of Eq. (8) as follows

$$\int_0^{q_{\rm uv}} \frac{qdq}{\varkappa_q q^2+\sigma} = \int_0^{q_{\rm uv}} \frac{dq}{\varkappa_q q} - \int_0^{q_{\rm uv}} \frac{\sigma dq}{(\varkappa_q q^2+\sigma)\varkappa_q q} \tag{S.14}$$

we get

$$\frac{\sigma}{\mu+\lambda} = \xi^2 - \xi_0^2 - \frac{T}{4\pi}\int_0^{\infty} dq \frac{\sigma}{(\varkappa_q q^2+\sigma)\varkappa_q q}, \tag{S.15}$$

(having in mind apply our theory to graphene, we put $d_c = 1$ here). The main contribution to this integral comes from small q that allowed us to extend upper limit of integration to infinity. Next, we interpolate the bending rigidity as

$$\varkappa_q = \varkappa\left(\frac{q+q_*}{q}\right)^{\eta}. \tag{S.16}$$

Assuming that $T \ll T_{\rm cr}$ and, consequently, $\xi - \xi_0 \ll \xi_0 \simeq 1$, we arrive after simple algebra at the following equation

$$\xi - \xi_0 = \frac{\sigma}{k_0} + \frac{T}{8\pi\varkappa} F\left(\frac{\sigma}{\sigma_1}\right), \tag{S.17}$$

where

$$\sigma_1 = \varkappa q_*^2 \sim \tilde{\mu} T/\varkappa, \tag{S.18}$$

and

$$F(x) = x\int_0^{\infty} \frac{dz}{z^{1-\eta}(1+z)^{\eta}\left[z^{2-\eta}(1+z)^{\eta}+x\right]} \propto \begin{cases} x^{\eta/(2-\eta)}, & \text{for} \quad x \to 0, \\ \ln x, & \text{for} \quad x \to \infty. \end{cases} \tag{S.19}$$

Since the numerical coefficient in Eq. (S.18) is unknown, we can rewrite the low-stress asymptotics of $F(x)$ in term of σ_* which is given by Eq. (11) of the main text and contains an unknown temperature-independent numerical coefficient $C \sim 1$. Hence, for $\sigma \ll \sigma_*$ we arrive at Eq. (10) of the main text, where in addition to the main anomalous contribution $\propto \sigma^{\alpha}$ we keep the subleading linear-in-σ term. For $\sigma \gg \sigma_0$, the linear term dominates. According to Eq. (S.19), the anomalous term is proportional to $\ln(\sigma/\sigma_*)$ in this region. However, since the anomalous term is subleading, one can use Eq. (10) of the main text in this region, too, if one is only interested in describing the leading behavior.

Renormalization group for disordered membrane with non-zero tension

For disordered case, one can perform calculations by using the replica trick. Replicating the fields $h_{\mathbf{q}} \to h^{(n)}_{\mathbf{q}}$ in the energy functional and omitting irrelevant constant, we obtain (see also Ref. [44]):

$$E^{\rm rep} = E_0^{\rm rep} + E_1^{\rm rep} + E_2^{\rm rep}, \tag{S.20}$$

where

$$E_0^{\rm rep} = \frac{1}{2}\sum_{n=1}^{n=N}\int (dq)\varkappa q^4 |\mathbf{h}^{(n)}_{\mathbf{q}} + \boldsymbol{\beta}_{\mathbf{q}}|^2, \tag{S.21}$$

$$E_1^{\rm rep} = \frac{L^2(\mu+\lambda)}{2}\sum_{n=1}^{n=N}\left(\xi^2 - 1 + \frac{K_n}{2}\right)^2, \tag{S.22}$$

$$E_2^{\rm rep} = \sum_{n=1}^{n=N}\frac{1}{4d_c} \times \int (dkdk'dq) R_{\mathbf{q}}(\mathbf{k},\mathbf{k}')\left(\mathbf{h}^{(n)}_{\mathbf{k}+\mathbf{q}}\mathbf{h}^{(n)}_{-\mathbf{k}}\right)\left(\mathbf{h}^{(n)}_{-\mathbf{k}'-\mathbf{q}}\mathbf{h}^{(n)}_{\mathbf{k}'}\right), \tag{S.23}$$

$$K_n = \int \frac{d^2x}{L^2}\partial_{\alpha}\mathbf{h}^{(n)}\partial_{\alpha}\mathbf{h}^{(n)}, \tag{S.24}$$

and index $n = 1,\ldots,N$ enumerates replicas (the rule of summation over repeated indices does not apply here). Next, we introduce auxiliary fields χ_n to decouple the zero-mode interaction in Eq. (S.22) and average $\exp(-E_{\rm rep}/T)$ with $P(\boldsymbol{\beta})$. In the absence of interaction $E_2^{\rm rep}$, the stationary phase conditions yield $\chi_1 = \ldots = \chi_N = i\sigma$, where tension σ and stretching factor ξ are connected by the following equation:

$$\frac{\sigma}{\mu+\lambda} = \xi^2 - 1 + \frac{d_c T}{4\pi}{\rm Tr}\left(\int_0^{q_*}\frac{qdq}{\hat{\varkappa}q^2+\sigma}\right). \tag{S.25}$$

Here we have introduced a replica-space matrix $\hat{\varkappa}$:

$$\hat{\varkappa} = \varkappa - \frac{b\varkappa^2}{T + b\varkappa N}\hat{J}, \tag{S.26}$$

where $\hat{J}$ is the matrix with all elements equal to unity: $J^{nm} = 1$. It is convenient to incorporate σ in the defini-

tion of the bending rigidity matrix by introducing

$$\hat{\varkappa}_{\mathbf{q}} = \varkappa + \frac{\sigma}{q^2} - \frac{b\varkappa^2}{T + b\varkappa N}\hat{J}. \tag{S.27}$$

The bare propagator is then a matrix in the replica space:

$$\hat{G}^0_{\mathbf{q}} = \frac{T\hat{\varkappa}^{-1}_{\mathbf{q}}}{q^4} = \frac{T}{\bar{\varkappa}_{\mathbf{q}} q^4}\left(1 + \bar{f}_{\mathbf{q}}\hat{J}\right), \tag{S.28}$$

$$\bar{\varkappa}_{\mathbf{q}} = \varkappa\frac{q^2 + q_\sigma^2}{q^2}, \quad \bar{f}_{\mathbf{q}} = f\frac{q^2}{q^2 + q_\sigma^2}. \tag{S.29}$$

Here we have introduced the dimensionless parameter [44]

$$f = \frac{b\varkappa}{T} \tag{S.30}$$

given by the ratio of the bare disorder, b, and the bare magnitude of dynamical (thermal) fluctuations, T/κ. The correlation function $\overline{\langle\partial_\alpha\mathbf{h}\partial_\alpha\mathbf{h}\rangle}$ in the harmonic approximation is given by $N^{-1}\mathrm{Tr}\hat{G}^0_{\mathbf{q}}$. (it worth noting that $\overline{\langle\partial_\alpha\mathbf{h}\partial_\alpha\mathbf{h}\rangle}$ can be calculated without replication, by the Gibbs averaging of $\partial_\alpha\mathbf{h}\partial_\alpha\mathbf{h}$ with the fluctuation energy E_0, where one should omit anharmonic terms).

Above we have neglected the anharmonic coupling, E_2^{rep}, so that $\varkappa$ and b were q-independent. In fact, the anharmonicity leads to a weak scale dependence of these variables: $\varkappa \to \varkappa_{\mathbf{q}}$, $b \to b_{\mathbf{q}}$, $f \to f_{\mathbf{q}}$. To find this dependence, we calculate the anharmonicity-induced self-energy $\hat{\Sigma}_{\mathbf{q}}$ and find the dressed Green function

$$\hat{G}_{\mathbf{q}} = \frac{T}{\hat{\varkappa}_{\mathbf{q}} q^4 + \hat{\Sigma}_{\mathbf{q}}}. \tag{S.31}$$

Next, we derive the RG equation for $\hat{\Sigma}_{\mathbf{q}}$ at the one-loop order (i.e., within RPA). The analysis is controlled by a parameter $1/d_c$ which is assumed to be small. We first calculate the polarization operator which becomes a replica-space matrix [44]:

$$\Pi^{nm}_{\mathbf{q}} = \frac{1}{3}\int (dk) k_\perp^4 G^{0,nm}_{\mathbf{k}} G^{0,nm}_{\mathbf{q}-\mathbf{k}} \tag{S.32}$$

$$= \frac{T^2}{3}\int (dk) k_\perp^4 \frac{(\hat{\varkappa}^{-1}_{\mathbf{k}})^{nm}}{k^4}\frac{(\hat{\varkappa}^{-1}_{\mathbf{q}-\mathbf{k}})^{nm}}{|\mathbf{q}-\mathbf{k}|^4}.$$

Here $\mathbf{k}_\perp = \hat{P}\mathbf{k} = \mathbf{k} - \mathbf{q}(\mathbf{kq})/q^2$, and $\hat{P}$ is the projection operator related to the transferred momentum $\mathbf{q}$,

$$P_{\alpha\beta} = \delta_{\alpha\beta} - q_\alpha q_\beta/q^2. \tag{S.33}$$

From Eqs. (S.28) and (S.32) we find

$$\hat{\Pi}_{\mathbf{q}} = \frac{T^2}{3}\int (dk) k_\perp^4 \frac{1 + \bar{f}_{\mathbf{k}} + \bar{f}_{\mathbf{q}-\mathbf{k}} + \hat{J}\bar{f}_{\mathbf{k}}\bar{f}_{\mathbf{q}-\mathbf{k}}}{\bar{\varkappa}_{\mathbf{k}} k^4 \bar{\varkappa}_{\mathbf{q}-\mathbf{k}}|\mathbf{q}-\mathbf{k}|^4}. \tag{S.34}$$

Using Eq. (S.29) we find that behavior of $\hat{\Pi}_{\mathbf{q}}$ is essentially different for $q \gg q_\sigma$ and $q \ll q_\sigma$:

$$\hat{\Pi}_{\mathbf{q}} = \frac{T^2}{16\pi\varkappa^2}\begin{cases} \dfrac{1}{q^2}\left(1 + 2f + f^2\hat{J}\right), & \text{for } q \gg q_\sigma, \\ \dfrac{1}{2q_\sigma^2}\left(1 + f + \dfrac{f^2}{12}\hat{J}\right), & \text{for } q \ll q_\sigma, \end{cases} \tag{S.35}$$

The upper ($q \gg q_\sigma$) asymptotics in Eq. (S.35) has been obtained previously in Ref. [44]. We assume that $q \ll q_*$ (relation between q and q_σ can be arbitrary), where the Ginzburg scale q_* is modified by disorder [44]:

$$q^* \sim \left[\frac{\tilde{\mu}T(1+2f)}{\varkappa^2}\right]^{1/2}. \tag{S.36}$$

It is worth noting that for strong disorder or low temperatures ($f \gg 1$) $q_* \sim (\tilde{\mu}b/\kappa)^{1/2}$ is independent of temperature, while for weak disorder ($f \ll 1$) , $q_* \propto T^{1/2}$. For such q, matrix elements of the self-energy in the replica space read

$$\Sigma^{nm}_{\mathbf{k}} = \frac{2T}{3d_c}\int (dq) k_\perp^4 \left(\hat{\Pi}^{-1}_{\mathbf{q}}\right)^{nm} G^{0,nm}_{\mathbf{k}-\mathbf{q}}. \tag{S.37}$$

Substituting here the bare Green function, Eq. (S.28), we find by simple power-counting that the corresponding integral diverges as $k^4 \ln k$ both for $k > q_\sigma$ and $k < q_\sigma$. This implies that RG equations can be written in terms of the renormalization of $\hat{\varkappa}$. Separating in thus obtained equation terms proportional to unity and to $\hat{J}$, we arrive to

$$\frac{1}{\varkappa}\frac{d\varkappa}{d\Lambda} = \eta\frac{1 + 3f + f^2}{(1+2f)^2}, \quad \frac{1}{f}\frac{df}{d\Lambda} = -\eta\frac{1+3f}{(1+2f)^2}. \tag{S.38}$$

Dynamical and static fluctuations in the flat phase. Flat phase 1 and flat phase 2

Here, we analyze the RG flows for $\varkappa$ and f at $q < \tilde{q}_\sigma$. The corresponding RG equations are analogous to the case $\sigma = 0$, yielding for $q \ll \tilde{q}_\sigma$

$$\frac{1}{\varkappa}\frac{d\varkappa}{d\Lambda} = -\frac{1}{f}\frac{df}{d\Lambda} = \eta\frac{12 + 12f - f^2}{6(1+f)^2}. \tag{S.39}$$

Note that $\varkappa f = \mathrm{const}$. Equations (S.39) have an unstable fixed point $f_{\mathrm{cr}} = 6 + 4\sqrt{3} \approx 12.9$. Thus, the flat phase can be separated into two parts: a phase where $\varkappa$ increases with the system size ($f < f_{\mathrm{cr}}$) and a phase where the membrane becomes softer at larger scales ($f > f_{\mathrm{cr}}$). The border between these phases can be found by using the fact that f_{cr} is numerically large. For $q \gg \tilde{q}_\sigma$, using the large-f asymptotic of the RG equation for f, we find that the border is given by the line $f = f_0 = \mathrm{const}$, where $f_0 = f_{\mathrm{cr}} + (3/4)\ln(q_*/\tilde{q}_\sigma)$, with q_* and $\tilde{q}_\sigma$ given

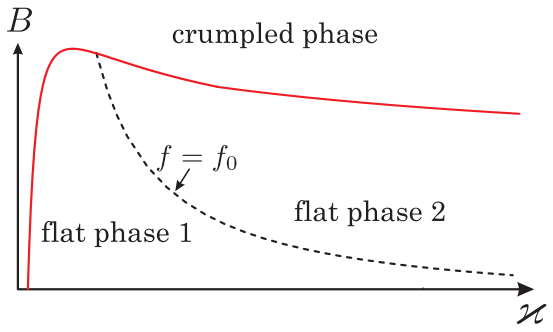

FIG. S1: Phase diagram of graphene in the plane of parameters $\varkappa$ (bending rigitidy) and B (disorder) at non-zero tension σ. The CT separating crumpled and flat phases is shown by full red line. Line $f = f_0$ separates two flat phases with different behavior of dynamical and static correlation functions.

by Eqs. (16) and (18) of the main text, respectively, see Fig. S1.

In both phases, $\varkappa_q q^2 \ll \sigma$, so that the scaling of $\varkappa$ is irrelevant for the CT and the membrane remains flat. The phases can be distinguished by the behavior of dynamical and static fluctuations. To characterize both types of fluctuations we introduce the corresponding correlation functions [33, 44]:

$$H^{\rm d}(x) = \overline{\langle \partial_\alpha \mathbf{h}(0) \partial_\alpha \mathbf{h}(\mathbf{x})\rangle} - H^{\rm s}(x), \qquad \text{(S.40)}$$

$$H^{\rm s}(x) = \overline{\langle \partial_\alpha \mathbf{h}(0)\rangle \langle \partial_\alpha \mathbf{h}(\mathbf{x})\rangle}. \qquad \text{(S.41)}$$

Here, $\langle \ldots \rangle$ stands for averaging over dynamical fluctuations in a given disorder realization, while the overbar means averaging over disorder. Functions $H_q^{\rm d}$ and $H_q^{\rm s}$ are given by the first and second term in Eq. (14) of the main text, respectively. For $q \ll \tilde{q}_\sigma$, we get

$$H_q^{\rm d} \approx \frac{d_c T}{\sigma}\left(1 - \frac{\varkappa_q q^2}{\sigma}\right), \qquad \text{(S.42)}$$

$$H_q^{\rm s} \approx \frac{d_c T f_q \varkappa_q q^2}{\sigma^2}\left(1 - \frac{2\varkappa_q q^2}{\sigma}\right). \qquad \text{(S.43)}$$

Here we keep corrections with respect to the small parameter $\varkappa q^2/\sigma$. Solving Eq. (23) of the main text, we find that the leading contributions to both dynamical and static functions are regular,

$$H_q^{\rm d(0)} = d_c T/\sigma = {\rm const}(q)$$

and

$$H_q^{\rm s(0)} = d_c T f_q \varkappa_q q^2/\sigma^2 \propto q^2,$$

each behaving in the same way for $f > f_{\rm cr}$ and $f < f_{\rm cr}$. However, the corrections show an anomalous scaling different in the two phases:

$$\delta H^{\rm d}_{q\to 0} = -\frac{d_c T}{\sigma^2}\varkappa_q q^2 \propto \begin{cases} q^{2-2\eta}, & \text{for } f < f_{\rm cr} \\ q^{2+\eta/6}, & \text{for } f > f_{\rm cr}, \end{cases}$$

$$\delta H^{\rm s}_{q\to 0} = -\frac{2 d_c T}{\sigma^3} f_q \varkappa_q^2 q^4 \propto \begin{cases} q^{4-2\eta}, & \text{for } f < f_{\rm cr} \\ q^{4+\eta/6}, & \text{for } f > f_{\rm cr}. \end{cases} \qquad \text{(S.44)}$$

These corrections are obtained by differentiating the correlation functions with respect to σ: $\delta H_q^{\rm d} = \partial(\sigma H_q^{\rm d})/\partial\sigma$, $\delta H_q^{\rm s} = \partial(\sigma^2 H_q^{\rm s})/\partial\sigma$. The difference in the behavior of the correlation functions (S.44) distinguishes the two flat phases, flat phase 1 and flat phase 2, shown in Fig. S1.

Comparison with numerical simulations of Ref. [46]

Here, we present some details on the comparison of our theory with numerical simulations for clean graphene presented in Ref. [46]. The simulations were performed for graphene samples of various sizes. Phenomenological formulas were found that fitted very well numerical data points in the considered range of stress and strain, see Eqs. (10), (11) of Ref. [46]. In our notations, these formulas become

$$k_{\rm eff} = \frac{2\xi[k_0/\xi_0 + CD(\xi - \xi_0)]}{1 + D(\xi - \xi_0)}, \qquad \text{(S.45)}$$

$$\sigma = \frac{2}{D}\left(\frac{k_0}{\xi_0} - C\right)\ln[1 + D(\xi - \xi_0)] + 2C(\xi - \xi_0), \qquad \text{(S.46)}$$

The parameters C, D, k_0, ξ_0 were found to be dependent on the system size L; this dependence was fitted by phenomenological formulas presented in Table I of Ref. [46]. For comparison with the theory, we used the values of these parameters for the sample of largest size (37888 atoms) considered in Ref. [46], since these numerical data should be less affected by finite-size effects.

Phenomenological equations (S.45) and (S.46) yield the implicit dependence of effective stiffness $k_{\rm eff}$ on σ, as found numerically in Ref. [46]. It is worth noting that $k_{\rm eff}$ does not go to zero at the point $\xi = \xi_0$ of zero strain (and zero stress). In other words, numerical simulations show the existence of small but finite linear stiffness $k_{\rm eff}(0)$. This is a finite-size effect: the power-law renormalization of effective stiffness is cut off by the system size. Indeed, the data of Ref. [46] also shows that this residual stiffness vanishes in the limit of large systems, $L \to \infty$. To compare the numerical data with our theoretical prediction for $k_{\rm eff}(\sigma)$ given by Eq. (19) of the main text (that corresponds to the thermodynamic limit), we have removed this finite-size effect by shifting Eq. (S.46) in such a way that the large-L condition $k_{\rm eff}(0) = 0$ is restored.